

Generalized Bloch states of a two-level atom in the field of counterpropagating waves:
application to the Kapitza–Dirac diffraction problem

This content has been downloaded from IOPscience. Please scroll down to see the full text.

2015 Phys. Scr. 90 115401

(<http://iopscience.iop.org/1402-4896/90/11/115401>)

View [the table of contents for this issue](#), or go to the [journal homepage](#) for more

Download details:

IP Address: 139.184.14.159

This content was downloaded on 05/05/2016 at 07:26

Please note that [terms and conditions apply](#).

Generalized Bloch states of a two-level atom in the field of counterpropagating waves: application to the Kapitza–Dirac diffraction problem

Gevorg Muradyan^{1,2} and Atom Zh Muradyan¹

¹Laboratory for Research and Modeling of Quantum Phenomena, Yerevan State University, Yerevan 0002, Armenia

²French Higher Institute of Engineering in Armenia, Yerevan 0037, Armenia

E-mail: gmurad@ysu.am

Received 19 January 2015, revised 13 July 2015

Accepted for publication 2 September 2015

Published 2 October 2015



CrossMark

Abstract

The Bloch-state approach to atomic translational states is extended out of adiabatic following and Raman–Nath approximations, taking into account the possible transfer of population from the initially populated internal energy level. The presented theory suggests a notion of potential energy corresponding to the initially populated internal state, and makes a generalization in the treatment of energy spectrum band-gap structure. Applying the theory to off-resonant Kapitza–Dirac diffraction and two-pulse standing wave atom interferometer (for the study of non-coherent processes in the cold atomic gases) we discuss the ability of the present approach for large-angle split multipath atom interferometry.

Keywords: atom interferometry, atom optics, quantum gases

(Some figures may appear in colour only in the online journal)

1. Introduction

In general, the problem of a composite particle in external field does not split into separate problems for internal and external degrees of freedom (see e.g. [1]). This problem, in particular, appears in one of the essential problems of contemporary atomic physics, namely, the behavior of atomic quantum states in a resonant field of laser radiation [2–5]. Here atomic translational and internal states appear interconnected. The reason for this entanglement is the fact that optical transitions between internal energy levels are invariably accompanied by changes in the momentum spectra. As a result, the quantum state equations digress from the Schrödinger-type, making general introduction of the notion of potential energy for each internal state or any combination of these states impossible even in case of simple two-level atoms [6]. The problem turns out to be exactly solvable only in case of a plane running wave, and the mentioned entanglement between the internal and translational states leads to a splitting

of energy-momentum dispersion relation into two intersecting subbranches [7, 8].

However in many applications, such as laser cooling and atom interferometry [9–12], we face, the challenge of having two counterpropagating waves as a laser field [13]. Approximate analytic solutions and corresponding potential energies here are known only for bordering far off-resonance (adiabatic following) [14, 15] and exact resonance [16] cases. For the adiabatic following case, the internal state population adiabatically stays on ground energy level and the atom behaves like a structureless particle. The exact resonance case is the contrary in a sense that potential energy is in line with symmetric and antisymmetric superpositions of two population probability amplitudes of internal energy levels. Both translational eigenfunctions are periodic Mathieu functions [17] with familiar energy bands and intervening energy gaps in their energy spectrum.

Scantiness of stationary solutions spreads to temporal solutions of the problem too. The evolution of translational

states in the field of counterpropagating waves, the so called near-resonant Kapitza–Dirac diffraction, is analytically tractable when the population of the upper internal energy level is ignorable during interaction or when the resonance is exact. It should be noted that time evolution problem is examined in momentum representation too, which allows one to bypass the above-mentioned stationary states in coordinate representation. Unfortunately, this approach compels one to ignore the kinetic energy term from the problem totally (see, for instance, [18]), or to discuss the problem in immediate proximity to this approximation [19, 20]. Being equivalent to immovable atoms approximation, this approach holds true for short interaction times only. That is, for timescales for which atomic displacement along the line of counterpropagating waves is short compared to the standing wave potential intensity modulation period (being a direct counterpart of thin grating Raman–Nath diffraction regime in optics [21], it acquired the Raman–Nath denomination). Another drawback of the approximation is that cancellation of kinetic energy in the Hamiltonian lifts restrictions conditioned by the conservation of energy, and thereby lifts restrictions on the magnitude of matterwaves’ splitting angles in the scattering problem. Lastly, Raman–Nath approximation, in analogy with the adiabatic following approximation, neglects the upper level population, which brings to the well-known Bessel-function representation for the diffraction probability amplitudes [11] (essential details are relegated to the appendix).

So, the present-day theory of the problem of a two-level atom in far off-resonant field of counterpropagating waves (standing wave), with or without restrictions on interaction times, totally neglects the transfer of population to the excited energy level. This paper reintroduces into the problem the (small, up to moderate) population transfers between internal states, developing a generalization of the Bloch theory for atomic states with a single-state population (see, e.g. [14, 22]). Derived stationary-state equation still keeps the Mathieu form, but a new interpretation of the energy zonal structure is introduced. As to potential energy, the notion holds true for the initially populated ground energy level.

This work was actually preceded by a search for possible schemes for multipath atom interferometry, a promising branch of light pulse atom interferometry [23], where higher sensitivity [24] can be secured by an increment of the interferometers’ enclosed area. As might have been expected, if the number of interfering paths is large, the resultant interferometric pattern may exhibit new and unexpected regularities even with small deviations from the applied approximation (in this case this means keeping the kinetic energy term and non-zero atomic excitation). Such a prospect in part has been confirmed in [25], arguing that accounting for upper level excitation in Raman–Nath approximation yields a number of interesting momentum distributions, absent in the familiar Bessel-function limit [26]. In the second part of this paper we take the next step in this direction, clarifying the ability of multipath interference (with discrete Gaussian distribution in the momentum space) as a beam splitter out of Raman–Nath approximation. Furthermore, basing on such a

splitting, we suggest and simulate a two-grating multipath interferometer, able to measure the temporal decay of coherence in cold atomic gas.

The paper is organized as follows: section 2 outlines the developed theory of translational stationary states of a two-level atom in the field of counterpropagating monochromatic waves. Approximation assumes large values of resonance detuning relative to atomic kinetic energy (in \hbar units) but not relative to total energy, as is assumed in the adiabatic following approximation. In section 3, the theory is applied to atomic Kapitza–Dirac diffraction problem to get appropriate for the multipath atom interferometry momentum distributions (acceptable switching times of interaction are also defined in this section). In section 4, we discuss a double-grating light-pulse atom interferometer sensitive to temporal evolution of coherency in the source of atoms and conclusions are drawn in section 5.

2. Translational stationary states of a two-level atom in the field of counterpropagating waves

We consider a two-level atom (of mass M) in an optical light grating formed by counterpropagating laser field waves of wavevector k , frequency $\omega = kc$ and amplitudes E_1 and E_2 :

$$E(z, t) = E_1 \exp(ikz - i\omega t) + E_2 \exp(-ikz - i\omega t) + \text{c.c.} \quad (1)$$

The transverse component of atomic center of mass (c.m.) motion is separated out in the problem and is irrelevant for the following discussion. Then the atomic state is treated by the following Schrödinger equation:

$$i\hbar \frac{\partial \Psi(z, \mathbf{r}, t)}{\partial t} = \left(-\frac{\hbar^2}{2M} \frac{\partial^2}{\partial z^2} + \widehat{H}_0(\mathbf{r}) - \widehat{d}E(z, t) \right) \Psi(z, \mathbf{r}, t), \quad (2)$$

where the first term in bracket is the 1D c.m. kinetic energy operator, $\widehat{H}_0(\mathbf{r})$ is the free atom Hamiltonian (in the c.m. frame) and \widehat{d} is the dipole moment operator.

$$\Psi(z, \mathbf{r}, t) = g(z, t) \psi_g(\mathbf{r}) \exp(-i\epsilon_g t/\hbar) + e(z, t) \psi_e(\mathbf{r}) \exp(-i\epsilon_e t/\hbar - i\Delta t) \quad (3)$$

is the mapping of wavefunction $\Psi(z, \mathbf{r}, t)$ on basis of ground and excited internal atomic states $\psi_g(\mathbf{r})$ and $\psi_e(\mathbf{r})$ ($\widehat{H}_0(\mathbf{r}) \psi_{g,e}(\mathbf{r}) = \epsilon_{g,e} \psi_{g,e}(\mathbf{r})$). Coefficient-functions $g(z, t)$ and $e(z, t)$ serve as wavefunctions of translational motion in the ground and excited internal states respectively, $\Delta = \omega - \omega_{\text{atom}}$ is the detuning of laser frequency ω from atomic transition frequency ω_{atom} .

Substitution of equations (1) and (3) into equation (2) yields the following pair of governing partial differential equations:

$$\left(i \frac{\partial}{\partial \tau} + \omega_r \frac{\partial^2}{\partial \eta^2} \right) g(\eta, \tau) = -(\zeta_1 e^{i\varphi_1} e^{i\eta} + \zeta_2 e^{i\varphi_2} e^{-i\eta}) e(\eta, \tau), \quad (4a)$$

$$\left(i \frac{\partial}{\partial \tau} + \text{sign} \Delta + \omega_r \frac{\partial^2}{\partial \eta^2} \right) e(\eta, \tau) = -(\zeta_1 e^{-i\varphi_1} e^{-i\eta} + \zeta_2 e^{-i\varphi_2} e^{i\eta}) g(\eta, \tau), \quad (4b)$$

where $\eta = kz$, $\tau = |\Delta| t$, $\zeta_{1,2} e^{i\varphi_{1,2}} = d^* E_{1,2} / \hbar |\Delta|$, $\omega_r = \hbar k^2 / 2M |\Delta|$ are the dimensionless coordinate, time, interaction energy and recoil frequency correspondingly, $d = \langle \psi_e | \hat{d} | \psi_g \rangle$ is the transition dipole moment. Translational and internal states are essentially entangled in equations (4a) and (4b). Spontaneous decay of atomic internal excitation as well as field polarizations are out of discussion.

The system (4a) and (4b) does not have exact analytic solutions in terms of known higher transcendental functions. Our approach to the problem solution contains only one stipulation: neglecting the kinetic energy operator term in equation (4b). It can be interpreted as condition of large resonance detuning relative to kinetic energy of atomic c.m. motion. The size of total energy, ingressed through the time derivative terms of equations, is clear of any assumptions. Thus we arrive to coupled equations

$$\left(i \frac{\partial}{\partial \tau} + \omega_r \frac{\partial^2}{\partial \eta^2} \right) g(\eta, \tau) = -(\zeta_1 e^{i\varphi_1} e^{i\eta} + \zeta_2 e^{i\varphi_2} e^{-i\eta}) e(\eta, \tau), \quad (5a)$$

$$\left(i \frac{\partial}{\partial \tau} + \text{sign} \Delta \right) e(\eta, \tau) = -(\zeta_1 e^{-i\varphi_1} e^{-i\eta} + \zeta_2 e^{-i\varphi_2} e^{i\eta}) g(\eta, \tau), \quad (5b)$$

where interaction parameters ζ_1 and ζ_2 are constant for monochromatic laser waves. Then, acting by operator $i \partial / \partial \tau + \text{sign} \Delta$ on equation (5a), one obtains a separate equation for the lower-level wave function $g(\eta, \tau)$:

$$\left(i \frac{\partial}{\partial \tau} + \text{sign} \Delta \right) \left(i \frac{\partial}{\partial \tau} + \omega_r \frac{\partial^2}{\partial \eta^2} \right) g(\eta, \tau) = (\zeta_1^2 + \zeta_2^2 + 2\zeta_1 \zeta_2 \cos(2\eta - \varphi)) g(\eta, \tau), \quad (6)$$

where $\varphi = \varphi_2 - \varphi_1$. Note that this is not a Schrödinger-type equation for $g(\eta, \tau)$ function and does not preserve the normalization condition for the $g(\eta, \tau)$ function only. Hence, unlike adiabatic following approximation, the present approach is characterized with a non-negligible transfer of population from one internal energy level to the other one during interaction. Equation (6) is the basis for the remainder of this paper.

The ansatz

$$\begin{aligned} g(\eta, \tau) &= g(\eta) \exp(-i\lambda\tau), \\ e(\eta, \tau) &= e(\eta) \exp(-i\lambda\tau) \end{aligned} \quad (7)$$

transforms the partial differential equation (6) into an ordinary differential equation

$$\left(\frac{d^2}{d\eta^2} + \mu - \frac{\zeta_1^2 + \zeta_2^2}{\omega_r(\text{sign} \Delta + \omega_r \mu)} - \frac{2\zeta_1 \zeta_2}{\omega_r(\text{sign} \Delta + \omega_r \mu)} \cos(2\eta - \varphi) \right) g(\eta) = 0, \quad (8)$$

where a new energy parameter $\mu \equiv \lambda / \omega_r$ is introduced. Without restrictions on generality, one can take $\varphi = 0$. It matches the origin of space coordinate η with one of the maxima of standing wave intensity. Mathematical structure of equation (8) coincides with the time-independent Schrödinger equation in the periodic potential and may be written, as usual, in the form of Mathieu equation

$$\left(\frac{d^2}{d\eta^2} + a - 2q \cos 2\eta \right) g(\eta) = 0, \quad (9)$$

where

$$\begin{aligned} a &= \mu - \frac{\zeta_1^2 + \zeta_2^2}{\omega_r(\text{sign} \Delta + \omega_r \mu)}, \\ q &= \frac{\zeta_1 \zeta_2}{\omega_r(\text{sign} \Delta + \omega_r \mu)}. \end{aligned} \quad (10)$$

Equation (9) has an essential disparity with respect to familiar applications in physics. It comes from the format in which energy appears in the equation. In ordinary physical applications energy is just the free coefficient a , while the coefficient q , which stands for the modulation depth of interaction, is energy independent. The structure of coefficients in definitions of (10) is different. The energy μ appears in parameter a in a nonlinear manner and participates in the determination of interaction parameter q . Thus we can state that the notion of atomic potential energy for the ground internal level is formally extendable out of adiabatic following approximation, taking into account non-vanishing excited level population. The ‘price’ for this is attribution of energy dependency to the potential.

The Bloch–Floquet theorem, as is well known, allows to take basic solutions of the Mathieu equation (9) in form

$$g(\eta) = \exp(iP\eta) f(\eta),$$

where $f(\eta)$ is a periodic function with period π . It should be chosen within the limits $[-\pi/2, \pi/2]$. Characteristic exponent P is the quasimomentum, dimensionless in case of equation (9) and is spread in the first Brillouin zone $[-1, 1]$. Two linear independent solutions named $ce(\eta, q)$ and $se(\eta, q)$, respectively, symmetric and antisymmetric relative to the origin $\eta = 0$, traditionally obey conditions $ce(0, q) = 1$, $ce'(0, q) = 0$ and $se(0, q) = 0$, $se'(0, q) = 1$ (prime is the derivative with respect to variable η) [17]. We introduce some coefficients in order to transform the normalization onto the unity length of variable η , convenient for quantum mechanical applications:

$$C(\eta, q) = k_c ce(\eta, q), \quad S(\eta, q) = k_s se(\eta, q). \quad (11)$$

Then the general solution to equation (9) may be written in the form

$$g(\mu; \eta) = A_c C(\eta, q) + A_s S(\eta, q), \quad (12)$$

where A_c and A_s are some energy-dependent coefficients.

The ordinary matching condition (at $\eta = \pi/2$) yields the following pair of homogeneous equations,

$$A_c (1 - e^{i\pi P})C(\pi/2, q) + A_s (1 + e^{i\pi P})S(\pi/2, q) = 0, \quad (13a)$$

$$A_c (1 + e^{i\pi P})C'(\pi/2, q) + A_s (1 - e^{i\pi P})S'(\pi/2, q) = 0. \quad (13b)$$

From the homogeneity of equations one gets the familiar form of dispersion relation,

$$\cos(\pi P) = \frac{C(\pi/2, q)S'(\pi/2, q) + S(\pi/2, q)C'(\pi/2, q)}{C(\pi/2, q)S'(\pi/2, q) - S(\pi/2, q)C'(\pi/2, q)}. \quad (14)$$

where the dimensionless energy μ enters through parameters a and q . Equation (14) determines the zonal structure of energy spectrum, where two limiting conditions $\cos(\pi P) = 1$ and $\cos(\pi P) = -1$ determine the borders between stable (allowed) and unstable (forbidden) solutions [17]. Each of these conditions is satisfied twice, and thereby four ‘types’ of border solutions are possible in general. Let us list them in the order of increasing energies:

(i) $\cos(\pi P) = 1$ at $C'(\pi/2, q) = 0$ ($S(\pi/2, q) \neq 0$). Then $A_c = 1, A_s = 0$ and $g(\mu; \eta) \Rightarrow C(\eta, q) = k_c \text{ce}(\eta, q)$. These represent the lower boundary of odd numbered energy bands $\nu = 1, 3, 5, \dots$

(ii) $\cos(\pi P) = -1$ at $S'(\pi/2, q) = 0$ ($C(\pi/2, q) \neq 0$), $A_c = 0, A_s = 1, g(\mu; \eta) \Rightarrow S(\eta, q) = k_s \text{se}(\eta, q)$. These represent the upper boundary of odd numbered energy bands $\nu = 1, 3, 5, \dots$

(iii) $\cos(\pi P) = -1$ at $C(\pi/2, q) = 0$ ($S'(\pi/2, q) \neq 0$), $A_c = 1, A_s = 0, g(\mu; \eta) \Rightarrow C(\eta, q) = k_c \text{ce}(\eta, q)$. These represent the lower boundary of even numbered energy bands $\nu = 2, 4, 6, \dots$

(iv) $\cos(\pi P) = 1$ at $S(\pi/2, q) = 0$ ($C'(\pi/2, q) \neq 0$), $A_c = 0, A_s = 1, g(\mu; \eta) \Rightarrow S(\eta, q) = k_s \text{se}(\eta, q)$. These represent the upper boundary of even numbered energy bands $\nu = 2, 4, 6, \dots$

Note that eigenfunctions $\text{ce}(\eta, q)$ and $\text{se}(\eta, q)$ for mentioned in (i)–(iv) border conditions become the Mathieu cosine and Mathieu sine functions $\text{ce}_{2r}(\eta, q), \text{se}_{2r+1}(\eta, q), \text{ce}_{2r+1}(\eta, q), \text{se}_{2r+2}(\eta, q), r = 0, 1, 2, \dots$, respectively.

Each energy band in the energy spectrum begins from lower energy boundary with a symmetric solution $C(\eta, q)$ and ends at the upper energy boundary with an antisymmetric solution $S(\eta, q)$. The difference from the familiar picture (see, e.g. [14]) refers to the geometrical interpretation of energy bands and energy gaps on the (q, a) plane. The parametric curve $a = a(q)$ (intersections of which with the borders of stability regions patterns the zonal structure of

energy spectrum) is not a straight line parallel to a -ordinate axis as it was in the familiar case. Now it is a curved line, and the width of any energy band (or gap) is determined as the length of the leg between the bottom and upper points of its intersection with the borders of the energy zone. In addition, the values on q -abscissa do not meet uniquely the depth of field intensity but are energy-dependent.

Hence, equation (12), with (13) and (14), concludes solution of the problem corresponding to internal ground energy level. Excited energy level solution follows immediately from equation (5b), subject to ansatz of equation (7).

3. Temporal solutions: application to near-resonant Kapitza–Dirac diffraction

We now turn to the solution of the temporal problem

$$g(\eta, \tau) = \sum_{\nu=1}^{\infty} \int_{-1}^1 K(P) g(\mu(P); \eta) \exp(-i\omega_r \mu \tau) dP, \quad (15)$$

bearing in mind its application to the problem of Kapitza–Dirac diffraction of a two-level atom [27–29] prepared in a discrete family of momentum states. Quasimomentum distribution $K(P)$ is specified through the initial spatial distribution $g(\eta, \tau = 0) \equiv g(\eta)$ (do not confuse the latter notation with the notation in equation (7)):

$$K(P) = \frac{1}{2\pi} \int_{-\infty}^{\infty} g^*(\mu(P); \eta) g(\eta) d\eta, \quad (16)$$

where the orthonormality condition

$$\int_{-\infty}^{\infty} g^*(\mu(P'); \eta) g(\mu(P); \eta) d\eta = 2\pi \delta(P' - P) \quad (17)$$

of eigenfunctions has been used. Inserting equation (16) into equation (15) we obtain the seeking wavefunctions’ general form:

$$g(\eta, \tau) = \frac{1}{2\pi} \sum_{\nu=1}^{\infty} \int_{-\infty}^{\infty} g(\eta) \times \left\{ \int_{-1}^1 g^*(\mu(P); \eta) g(\mu(P); \eta) \times \exp(-i\omega_r \mu(P)\tau) dP \right\} d\eta. \quad (18)$$

Note that sometimes it is convenient to take the integral over the energy space, instead of quasimomentum one. Then the transformation formula $dP = (1 - f^2(\mu))^{-1/2} \text{Abs} \left[\frac{df(\mu)}{d\mu} \right] d\mu$ has to be used, with $f(\mu)$ being the right-hand side of equation (14).

Corresponding to the excited energy level solution is obtained by a simple integration of equation (5b):

$$e(\eta, \tau) e^{-i\tau \text{sign} \Delta} = e(\eta, 0) - (\zeta_1^* e^{-i\eta} + \zeta_2^* e^{i\eta}) \int_0^{\tau} e^{i\tau' \text{sign} \Delta} g(\eta, \tau') d\tau', \quad (19)$$

where $g(\eta, \tau')$ already is a known function of time.

Let us now apply these results to the problem of near-resonant Kapitza–Dirac diffraction, where a two-level atom for a limited time τ scatters on an optical lattice of near-resonant frequency. The atom is assumed initially to be prepared in a discrete Gaussian superposition of momentum states and residing on the ground energy level:

$$g(\eta) = e^{i\eta_0 \eta} \sum_{l=-\infty}^{\infty} \frac{1}{\pi^{1/4} \sigma^{1/4}} e^{i2l\alpha - l^2/2\sigma} e^{i2l\eta},$$

$$e(\eta, 0) = 0. \tag{20}$$

It is periodically modulated in space, shares the $\lambda/2$ -period of the field intensity and thus can be realized by slowly loading a Bose–Einstein condensate (BEC) into the optical lattice. Parameter p_g denotes the mean value of initial momentum (in units of $\hbar k$), while the second parameter α specifies the spatial shift of incident matter-wave distribution pattern relative to the diffracting lattice distribution pattern. The latter one plays, as expected, a dominant role in formation of diffraction picture. Substituting this distribution into equation (18) yields the following compact analytical expressions

$$g(\eta, \tau) = \sum_{\nu=1}^{\infty} \left(\frac{1}{\pi} \int_{-\pi/2}^{\pi/2} g^*(\mu_\nu; \eta') g(\eta') d\eta' \right) \times g(\mu_\nu; \eta) \exp(-i\omega_r \mu_\nu \tau), \tag{21}$$

$$e(\eta, \tau) e^{-i\tau \text{sign}\Delta} = -(\zeta_1^* e^{-i\eta} + \zeta_2^* e^{i\eta}) \times \sum_{\nu=1}^{\infty} \left(\frac{1}{\pi} \int_{-\pi/2}^{\pi/2} g^*(\mu_\nu; \eta') g(\eta') d\eta' \right) \times g(\mu_\nu; \eta) \frac{\exp(-i(\text{sign}\Delta + \omega_r \mu_\nu)\tau) - 1}{\text{sign}\Delta + \omega_r \mu_\nu} \tag{22}$$

for the state functions. $\mu_\nu \equiv \mu$ (at $P = p_g$ in ν -th energy band) is a shortcut notation, extracting a discrete set of values from the energy band spectrum.

We will restrict ourselves to the important case $p_g = 0$, i.e., perpendicular incidence of matter wave on the optical lattice. Then the contributing set of energy levels are situated at the $P = 0$ borders of energy bands and correspond to the above-mentioned cases (i) and (iv). First of them pertains to the odd numbered energy bands and the second one—to the even numbered energy bands. As the summation in equations (21) and (22) is split into two families with odd and even $\nu - s$ we come to

$$g(\eta, \tau) = \sum_{\text{odd}\nu} \left(\frac{1}{\pi} \int_{-\pi/2}^{\pi/2} C^*(\eta', q_\nu) g(\eta') d\eta' \right) \times C(\eta, q_\nu) e^{-i\omega_r \mu_\nu \tau} + \sum_{\text{even}\nu} \left(\frac{1}{\pi} \int_{-\pi/2}^{\pi/2} S^*(\eta', q_\nu) g(\eta') d\eta' \right) \times S(\eta, q) e^{-i\omega_r \mu_\nu \tau}, \tag{23}$$

$$e(\eta, \tau) e^{-i\tau \text{sign}\Delta} = -(\zeta_1^* e^{-i\eta} + \zeta_2^* e^{i\eta}) \times \sum_{\text{odd}\nu} \left(\frac{1}{\pi} \int_{-\pi/2}^{\pi/2} C^*(\eta', q_\nu) g(\eta') d\eta' \right) \times C(\eta, q_\nu) \frac{e^{-i(\text{sign}\Delta + \omega_r \mu_\nu)\tau} - 1}{\text{sign}\Delta + \omega_r \mu_\nu} - (\zeta_1^* e^{-i\eta} + \zeta_2^* e^{i\eta}) \times \sum_{\text{even}\nu} \left(\frac{1}{\pi} \int_{-\pi/2}^{\pi/2} S^*(\eta, q_\nu) g(\eta') d\eta' \right) \times S(\eta, q_\nu) \frac{e^{-i(\text{sign}\Delta + \omega_r \mu_\nu)\tau} - 1}{\text{sign}\Delta + \omega_r \mu_\nu}. \tag{24}$$

We are interested in momentum distributions given by $g_n(\tau) = \frac{1}{\pi} \int_{-\pi/2}^{\pi/2} g(\eta, \tau) e^{-i2n\eta} d\eta$ and $e_n(\tau) e^{-i\tau \text{sign}\Delta} = \frac{1}{\pi} \int_{-\pi/2}^{\pi/2} e^{-i\tau \text{sign}\Delta} e(\eta, \tau) e^{-i(2n+1)\eta} d\eta$ probability amplitudes, which now will have the form

$$g_n(\tau) = \frac{1}{\pi} \int_{-\pi/2}^{\pi/2} g(\eta, \tau) e^{-i2n\eta} d\eta = \sum_{\text{odd}\nu} \left(\frac{1}{\pi} \int_{-\pi/2}^{\pi/2} C^*(\eta, q_\nu) g(\eta) d\eta \right) \times \left(\frac{1}{\pi} \int_{-\pi/2}^{\pi/2} C(\eta, q_\nu) e^{-im\eta} \right) e^{-i\omega_r \mu_\nu \tau} + \sum_{\text{even}\nu} \left(\frac{1}{\pi} \int_{-\pi/2}^{\pi/2} S^*(\eta, q_\nu) g(\eta) d\eta \right) \times \left(\frac{1}{\pi} \int_{-\pi/2}^{\pi/2} S(\eta, q_\nu) e^{-im\eta} \right) e^{-i\omega_r \mu_\nu \tau}, \tag{25}$$

and

$$e_n(\tau) = \frac{1}{\pi} \int_{-\pi/2}^{\pi/2} e(\eta, \tau) e^{-i(2n+1)\eta} d\eta = \sum_{\text{odd}\nu} \left(\frac{1}{\pi} \int_{-\pi/2}^{\pi/2} C^*(\eta, q_\nu) g(\eta) d\eta \right) \times \left(\frac{1}{\pi} \int_{-\pi/2}^{\pi/2} (\zeta_1^* e^{-i\eta} + \zeta_2^* e^{i\eta}) \right) \times C(\eta, q_\nu) e^{-im\eta} + \sum_{\text{even}\nu} \left(\frac{1}{\pi} \int_{-\pi/2}^{\pi/2} S^*(\eta, q_\nu) g(\eta) d\eta \right) \times \left(\frac{1}{\pi} \int_{-\pi/2}^{\pi/2} (\zeta_1^* e^{-i\eta} + \zeta_2^* e^{i\eta}) \right) \times S(\eta, q_\nu) e^{-im\eta} \times \frac{e^{-i(\text{sign}\Delta + \omega_r \mu_\nu)\tau} - 1}{\text{sign}\Delta + \omega_r \mu_\nu}. \tag{26}$$

It has to be noted that equations (25) and (26) are applicable not only for the initial distribution of equation (20) but for any incident distribution $g(\eta)$ which has the same periodicity as the diffracting optical potential.

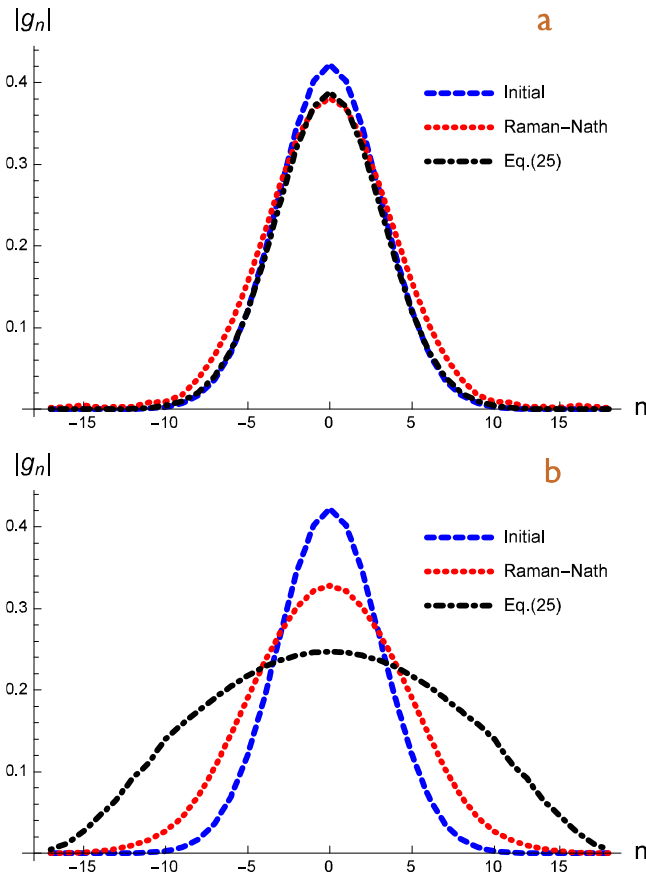


Figure 1. Momentum distributions for (a) short and (b) intermediate interaction times (with $\alpha = 0$) for the ground internal energy level. The dashed line (blue) corresponds to the initial distribution, the dotted line (red) correspond to the Raman-Nath approximation (see the appendix) and the dot-dashed line (black) gives the distribution corresponding to equation (25). In the presented approximation the expansion of momentum distribution stops for long interaction times due to energy conservation, while in the Raman-Nath approximation it continues. Atomic momenta on the horizontal axis are in units of photon recoil momentum $\hbar k$. The parameter values are $\xi_1 = \xi_2 = \sqrt{0.02}$, $\sigma = 10$ and $\tau = 100$ and $\tau = 300$ for figures 1(a) and (b) correspondingly. In case of ^{23}Na atoms with resonance detuning $\Delta = 10^{10}$ Hz they yield $E = 5 \times 10^4 \text{ V m}^{-1}$, $t \approx 10^{-7} - 10^{-8}$ s, quite permissible in present-day atomic physics laboratories.

Near-resonant Kapitza-Dirac diffraction with a discrete-Gaussian initial distribution has earlier been studied in Raman-Nath approximation and the study led to a monotone expansion of momentum distribution [26] as well as to its two-bunch splitting [25], providing an opportunity to be of a practical interest for multipath atom interferometry. Our numerical calculations, implemented on the basis of equations (25) and (26) confirm the mentioned results only for short interaction times. For longer times the picture is different: the momentum expansion stops (due to energy conservation in our theory) and makes slow oscillations with scaling up irregularities in the distribution picture. Note that such timing for Kapitza-Dirac diffraction is well known in case of single-momentum incident beam and has been predicted based on numerical solutions in [28–30], and observed

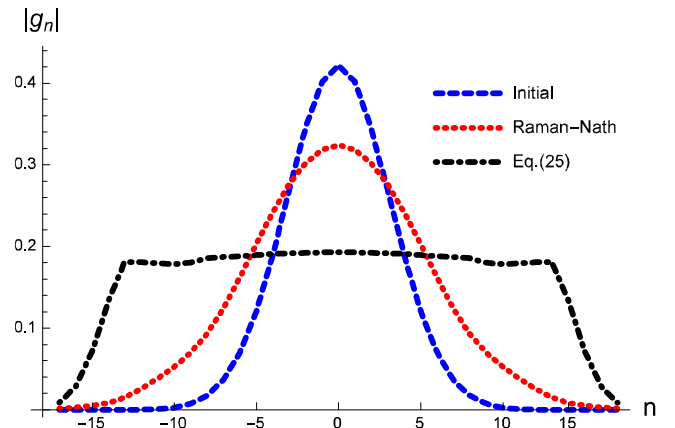


Figure 2. Momentum distributions, as in figure 1, at $\tau = 400$ when the momentum distribution given by equation (25) gets the maximum allowed width.

experimentally in [31, 32]. This assures a high quality position for the present approximation in the diffraction problem.

Figures 1(a) and (b) compare Raman-Nath and presented in equations (25) and (26) approximations. Phase shift parameter α is taken as null, i.e. no spatial shift of incident matter wave modulation relative to the diffracting field intensity modulation is assumed. In the case of this geometry, the main attribute is the broadening of momentum distribution. A difference relative to Raman-Nath approximation appears even in short time limit: the momentum distribution in fact expands more rapidly. This is a new and welcome ascertainment from the viewpoint of experimental implementations.

It is interesting that the first stage of momentum expansion goes to a table-size form, as in figure 2. This is the maximum expansion size possible. For longer times, as noted earlier, the oscillation distribution gradually yields a chaotic pattern.

3.1. To the smoothness of light-pulse envelopes

The presented approach assumes instantaneous switching of interaction. It effectively breaks the interaction adiabaticity and thereby creates favorable conditions for creating high orders in the atomic diffraction spectrum. Indeed, any redistribution in the momentum space automatically means a corresponding quantum transition between the translational energy levels, demanding thereby a failure of adiabaticity in the state evolution. As the grain of translational energy is the recoil energy $\epsilon_{\text{recoil}} = \hbar^2 k^2 / 2M$, largely separated momentum states can be expected only if $\delta\epsilon \gg \epsilon_{\text{recoil}}$ [19, 33], where $\delta\epsilon$ is the energy uncertainty associated with laser linewidth, $\delta\omega_{\text{laser}}$, the inverse of the characteristic switching time T . Of practical interest is the order of ratio $\epsilon_{\text{recoil}} / \delta\epsilon$ that provides the applicability of the stepwise approximation. To examine this question, we apply to a quite flexible envelope form

$$\xi_{1,2}(\tau) = \frac{\xi_{1,2}}{1 + e^{-\tau/|\Delta|T_i}} \theta(\tau_i - \tau) + \frac{\xi_{1,2}}{1 + e^{(\tau-\tau_f)/|\Delta|T_f}} \theta(\tau - \tau_i), \quad (27)$$

where T_i and T_f characterize the switching on and switching off of the interaction, τ_i and τ_f are durations before and after the pulse peak value is achieved, respectively. The Raman–Nath approximation of the two-level problem [34] gives enough grounding to handle the problem. It ensures that the stepwise approximation is acceptable above the value 10^3 for the inverse of parameter $\epsilon_{\text{recoil}}/\delta\epsilon = \omega_{\text{recoil}} |\Delta| T_{i,f}$. Below it, the momentum expansion is gradually cancelled and near the value ten loses interferometric attractiveness.

4. Simulation of a double-grating multipath atom interferometer

Now we proceed to a scheme of a two-pulse multipath atom interferometer [35, 36], with qualitatively new features that arise in the discussed case. The cold atomic gas is assumed to be initially prepared in Gaussian superposition of discrete momentum states using standing wave periodic potential of a consistent depth in a wide-spread and shallow time-orbiting potential trap. The interferometric part presents a pair of pulsed standing waves (composed of counterpropagating waves) separated by a variable delay time and applied to the matter wave of the atomic cloud. The first pulsed standing wave (as a phase grating) transforms the initial wave packet into a new family of momentum states, as described previously in section 3. The second pulsed standing wave splits each of these momentum states. Thus, the probability of having atoms in any given final momentum states is a result of interference of many momentum-space paths. Simultaneously with the second standing wave, the trapping potential is switched off from the interaction picture and after free time-of flight expansion for few milliseconds, the resultant momentum components no longer overlap in the coordinate space and are assumed to be imaged by resonant absorption imaging.

So, the principal stage of the inferred atomic interferometer is composed of two parts: first is the effect of standing wave pulses on prepared atomic matter wave and second is the atomic matter wave time evolution between interactions with standing wave pulses. For more specific discussion we assume that the object of our interferometer is measurement of characteristic times of decoherence in the cold atomic sample. As will be concretized later, durations of both pulsed standing waves are much shorter than the anticipated times of decoherency, and it enables us to employ equations (25) and (26) to scattering processes. Decoherence shows itself between the pulses and may be modelled as free from the trapping potential in the adopted shallow potential approximation.

Our numerical simulations are carried out for sodium $\lambda_L = 589$ nm line (corresponding recoil frequency $\hbar k^2/2M$ equals $2\pi \cdot 25$ kHz). Each standing wave pulse being detuned by $\Delta/2\pi = -600$ MHz from the optical transition, preserves the coherency during the diffraction [37]. The first pulse's duration is 65 nanoseconds (corresponding to $\tau_1 = 246$), which is out of Raman–Nath approximation at least for $n \geq 4$ momentum states. To be coherent in the intermediate stage,

the corresponding state function $g(\eta, \tau)$ of single-atom approximation can be written in the following free evolution form:

$$g_{\text{coherent}}(\eta, \tau) = \sum_{n=-\infty}^{\infty} G_n e^{i n \eta} \exp(-i 4n^2 \omega_r \tau), \quad (28)$$

where $\tau = 0$ is the start point of the intermediate stage, and $G_n = g_n(\tau_1)$ is the momentum state amplitude immediately after application of the first pulse (see equation (25)). So each momentum state acquires completely deterministic phases $\exp(-i 4n^2 \omega_r \tau)$ during the evolution. It is important for our interferometric proposal that the wavefunction temporally can be reconstructed at multiples of $\tau_T = \pi/2\omega_r$, the well known Talbot time of pattern replication in dimensionless units. In our case, $t_T = |\Delta| \tau_T = 10 \mu\text{s}$ and is much smaller than the characteristic decoherence time of a laser cooled atomic gas about the BEC transition temperature which is of the order of milliseconds. And the last but a key point. If the length of the intermediate stage is taken $\tau_0 = 1430$ (corresponding to about $2.4 \mu\text{s}$) then after diffraction on the second standing wave pulse, all odd diffraction orders disappear. This is a specific result for multipath interference in momentum space and assumes maintenance of coherency in all stages of evolution. In this idealized case after each Talbot time added to the intermediate stage longer periodic picture will be formed. However, the presence of decoherency increasing the dephasing between the momentum states should gradually yield fringe blurring as a diffusion-type equalization of populations in adjacent odd and even diffraction orders. The minimal intermediate time τ_0 is much smaller than the expected time τ_d of decoherence and thus can be used as the reference measurement point. Ensuring this, our method supposes to go ahead with Talbot interval steps τ_T up to chaotic equalization of even and odd order populations.

To include decoherency into the theory, we introduce a phase-factor $e^{i\alpha}$ in the probability amplitude G_n of equation (28). For the real-valued parameter α is chosen a partition law $\alpha = r \exp(-r^2/2R^2)$, where r is a random number uniformly distributed in the range $[-\pi, \pi]$. The influence of decoherency is taken into account through the width parameter R , taking it growing with the lapse of time, for instance, linearly: $R = R_0 + \tau/\tau_{\text{rate}}$ with some $R_0 \ll 1$ and characteristic time $\tau_{\text{rate}} = 100 \tau_T$ (1 ms in physical units). Our numerical calculations confirm the principal ability of the present scheme of atom interferometer to watch over the decoherency in the laser cooled atomic gases and to determine the characteristic time, connecting it with the introduced in the theory parameter τ_{rate} , and gives us a value $\tau_d \approx 4.5 \div 5 \tau_{\text{rate}}$.

5. Summary

We presented an analytic approximation for the translational stationary states of a two-level atom in the field of laser counterpropagating waves. It is beyond the familiar Raman–Nath and adiabatic following approximations owing to acceptance of some transfer of population between the

internal energy levels. The problem of eigenstates is formulated and solved within the limits of Mathieu equation with a ‘curvilinear’ treatment of the band structure of the energy spectrum. For relatively short interaction times, the theory justifies earlier obtained results about the two-bunch momentum splitting and monotonic expansion of initial discrete-Gaussian distribution in the field of off-resonant counterpropagating waves. For longer interaction times the energy conservation comes into play, restricting the size of spreading momentum states due to diffraction. The advantage of the present theory to be used in the modelling of multipath atom interferometers is justified, applying it to the problem of incoherence in laser cooled atomic gases.

Acknowledgments

This work was supported by Armenian State Committee of Science and Armenian National Science and Education fund grant nano-3488.

Appendix A. Raman–Nath and adiabatic following approximations

The Raman–Nath approximation is regarded as neglect of kinetic energy term $-\omega_r \partial^2/\partial\eta^2$ in all probability amplitude equations. Then, differential equation (6) with partial derivatives transforms into a second order ordinary differential equation with respect to time τ , thereby transforming the spatial coordinate η into a parameter of equation. It is easily solved to yield two characteristic values (see ansatz (7))

$$\begin{aligned}\lambda_1(\eta) &= -\frac{\text{sign}\Delta}{2} + \sqrt{\frac{1}{4} + \zeta_1^2 + \zeta_2^2 + 2\zeta_1\zeta_2 \cos 2\eta}, \\ \lambda_2(\eta) &= -\frac{\text{sign}\Delta}{2} - \sqrt{\frac{1}{4} + \zeta_1^2 + \zeta_2^2 + 2\zeta_1\zeta_2 \cos 2\eta}.\end{aligned}\quad (\text{A.1})$$

Then temporal evolution of the ground and excited states read as

$$g(\eta, \tau) = g_1(\eta)\exp(-i\lambda_1(\eta)\tau) + g_2(\eta)\exp(-i\lambda_2(\eta)\tau), \quad (\text{A.2})$$

$$\begin{aligned}e(\eta, \tau) &= -\left(\zeta_1 e^{-i\eta} + \zeta_2 e^{i\eta}\right) \\ &\times \left(g_1(\eta) \frac{e^{-i\lambda_1(\eta)\tau}}{\text{sign}\Delta + \lambda_1(\eta)} \right. \\ &\left. + g_2(\eta) \frac{e^{-i\lambda_2(\eta)\tau}}{\text{sign}\Delta + \lambda_2(\eta)} \right),\end{aligned}\quad (\text{A.3})$$

where $g_1(\eta)$ and $g_2(\eta)$ have to be determined from initial conditions $g(\eta, \tau = 0) = g(\eta)$ and $e(\eta, \tau = 0) = e(\eta)$:

$$\begin{aligned}g_1(\eta) &= -\frac{g(\eta)\lambda_2(\eta) + (\zeta_1 e^{i\eta} + \zeta_2 e^{-i\eta}) e(\eta)}{\lambda_1(\eta) - \lambda_2(\eta)}, \\ g_2(\eta) &= \frac{g(\eta)\lambda_1(\eta) + (\zeta_1 e^{i\eta} + \zeta_2 e^{-i\eta}) e(\eta)}{\lambda_1(\eta) - \lambda_2(\eta)},\end{aligned}\quad (\text{A.4})$$

Corresponding to Raman–Nath approximation curves in figure 1 are drawn using equation (A.2).

The referred second, adiabatic following, approximation is regarded as the omission of the time derivative term in equation (4b) or, which is the same, in the first bracket in equation (6). Approximation is allowed when the detuning energy strongly exceeds the kinetic and total energies of the atomic translational motion. The excited state now becomes non-relevant, while the governing equation for the ground state amplitude takes the Schrödinger-type form,

$$\begin{aligned}i \frac{\partial}{\partial \tau} g(\eta, \tau) \\ = \left(-\omega_r \frac{\partial^2}{\partial \eta^2} + \frac{1}{\text{sign}\Delta} (\zeta_1^2 + \zeta_2^2 + 2\zeta_1\zeta_2 \cos 2\eta) \right) g(\eta, \tau).\end{aligned}\quad (\text{A.5})$$

It solely holds the normalization condition. All relevant formulas hold true by nulling the summand $\omega_r \mu$ at the term $\text{sign}\Delta$ starting from equation (10). Particularly, the energy zone structure obtains the familiar interpretation.

These approximations are often used jointly and are termed in short as Raman–Nath approximation. This picture gives a clear physical picture and utmost simplification of mathematical forms in both space and momentum representations. Really, additional neglect of spatial derivative term in equation (A.5) results in a pure phase modulation for the probability amplitude $g(\eta, \tau)$. Then in the momentum representation one gets the well known Bessel function form

$$g_m(\tau) = i^m J_m \left(\frac{2\zeta_1\zeta_2\tau}{\text{sign}\Delta} \right),$$

where argument is the number of transitions between internal energy levels during interaction. It should be noted, in any case, that the compact character of this expression makes it very attractive and somewhat obscures its narrow validity range, as is apparent from the above analysis. The formula shows also a nice regularity about the constant $(\pi/2)$ phase differences between the neighboring diffraction orders. Such a regularity with an arbitrary constant α has been used in initial Gaussian distribution of equation (23).

References

- [1] Messiah A 1967 *Quantum Mechanics* vol 1 (Amsterdam: North-Holland) p 363
- [2] Foot C J 2005 *Atomic Physics* (Oxford: Oxford University Press) p 11 ch 9
- [3] Demtröder W 2006 *Atoms, Molecules and Photons* (Berlin: Springer) ch 12
- [4] Le Bellac M 2006 *Quantum Physics* (Cambridge: Cambridge University Press) ch 14
- [5] Walls D F and Milburn G J 2010 *Quantum Optics* (Berlin: Springer) ch 17
- [6] Allen L and Eberly J H 1975 *Optical Resonance and Two-Level Atoms* (New York: Wiley)
- [7] Pusep A Y, Doktorov A B and Burshtein A I 1977 *Zh. Eksp. Teor. Fiz.* **72** 98
- [8] Borde C J and Lammerzahl C 1999 *Ann. Phys., Lpz.* **1** 83

- [9] Metcalf H J and van der Straten P 1999 *Laser Cooling and Trapping* (New York: Springer)
- [10] Berman P R (ed) 1997 *Atom Interferometry* (San Diego, CA: Academic)
- [11] Cronin A D, Schmiedmayer J and Pritchard D E 2009 *Rev. Mod. Phys.* **81** 1051
- [12] Müller H 2014 *Atom interferometry Proc. Int. School of Physics Enrico Fermi, Course CLXXXVIII* ed G M Tino and M A Kasevich (Amsterdam: IOS Press)
- [13] Compagno G, Peng J S and Persico F 1982 *Phys. Rev. A* **26** 2065
- [14] Horne M, Jex I and Zeilinger A 1999 *Phys. Rev. A* **59** 2190
- [15] O'Dell D H J 2001 *J. Phys. A* **34** 3897
- [16] Minogin V G and Letokhov V S 1987 *Laser Light Pressure on Atoms* (New York: Gordon and Breach) p 203
- [17] Abramowitz M and Stegun I A 1975 *Handbook of Mathematical Functions* (New York: Dover) p 725
- [18] Cook R J and Bernhardt A F 1978 *Phys. Rev. A* **18** 2533
- [19] Mueller H, Chiow S W and Chu S 2008 *Phys. Rev. A* **77** 023609
- [20] Simula T P, Muradyan A and Molmer K 2007 *Phys. Rev. A* **76** 063619
- [21] Born M and Wolf E 1970 *Principles of Optics* (Oxford: Pergamon) p 609
- [22] Champenois C, Buchner M, Delhuille R, Mathevet R, Robilliard C, Rizzo C and Vigue J 2001 *Eur. Phys. J. D* **13** 271
- [23] Barrett B, Chan I, Mok C, Carew A, Yavin I, Kumarakrishnan A, Cahn S B and Sleator T 2011 *Adv. At. Mol. Opt. Phys.* **60** 119
- [24] Chiow S W, Kovacy T, Chein H-C and Kasevich M A 2011 *Phys. Rev. Lett.* **107** 130403
- [25] Hovhannisyan L and Muradyan A Z 2012 *J. Phys. Conf. Ser.* **350** 012011
- [26] Ishkhanyan A M 2000 *Phys. Rev. A* **61** 063611
- [27] Arutyunyan V M and Muradyan A Z 1975 *Rep. Acad. Sci. Arm. SSR* **60** 275 (in Russian)
- [28] Bernhardt A F and Shore B W 1981 *Phys. Rev. A* **23** 1290
- [29] Martin P J, Gould P L, Oldaker B J, Miklich A H and Pritchard D E *Phys. Rev. A* **36** 2495
- [30] Janicke U and Wilkens M 1994 *Phys. Rev. A* **50** 3265
- [31] Ovchinnikov Y B, Muller J H, Doery M R, Vredendregt E J D, Helmerson K, Rolston S L and Phillips W D 1999 *Phys. Rev. Lett.* **83** 284
- [32] Gadway B, Pertot D, Reimann R, Cohen M G and Schneble D 2009 *Opt. Express* **17** 19173
- [33] Keller C, Schmiedmayer J, Zeilinger A, Nonn T, Durr S and Rempe G 1999 *Appl. Phys. B* **69** 303
- [34] Nikitin E E 1962 *Opt. Spectrosc.* **13** 431
- [35] Edwards M, Benton B, Heward J and Clark C W 2010 *Phys. Rev. A* **82** 063613
- [36] Li W, He T and Smerzi A 2014 *Phys. Rev. Lett.* **113** 023003
- [37] Deng L, Hegley E W, Denschlag J, Simsarian J E, Edwards M, Clark C W, Helmerson K, Rolston S L and Phillips W D 1999 *Phys. Rev. Lett.* **83** 5407